Tellus (2007), 59B, 919–936
Printed in Singapore. All rights reserved

TELLUS

Vertical variability and effect of stability on turbulence characteristics down to the floor of a pine forest

By SAMULI LAUNIAINEN[1]*, TIMO VESALA[1], MEELIS MÖLDER[2], IVAN MAMMARELLA[3], SAMPO SMOLANDER[3], ÜLLAR RANNIK[1], PASI KOLARI[4], PERTTI HARI[4], ANDERS LINDROTH[2] and GABRIEL G. KATUL[5], [1]*Department of Physical Sciences, P.O. Box 64, FIN-00014, University of Helsinki, Finland;* [2]*Department of Physical Geography and Ecosystem Analysis, Sölvegatan 13, SE-22362 Lund University, Sweden;* [3]*Department of Physical Sciences, P.O. Box 68, FIN-00014, University of Helsinki, Finland;* [4]*Department of Forest Ecology, P.O. Box 27, FIN-00014, University of Helsinki, Finland;* [5]*Nicholas School of the Environment and Earth Sciences, Box 90328, Duke University, Durham, North Carolina*

(Manuscript received 30 November 2006; in final form 1 July 2007)

ABSTRACT

Among the fundamental problems in canopy turbulence, particularly near the forest floor, remain the local diabatic effects and linkages between turbulent length scales and the canopy morphology. To progress on these problems, mean and higher order turbulence statistics are collected in a uniform pine forest across a wide range of atmospheric stability conditions using five 3-D anemometers in the subcanopy. The main novelties from this experiment are: (1) the agreement between second-order closure model results and measurements suggest that diabatic states in the layer above the canopy explain much of the modulations of the key velocity statistics inside the canopy except in the immediate vicinity of the trunk space and for very stable conditions. (2) The dimensionless turbulent kinetic energy in the trunk space is large due to a large longitudinal velocity variance but it is inactive and contributes little to momentum fluxes. (3) Near the floor layer, a logarithmic mean velocity profile is formed and vertical eddies are strongly suppressed modifying all power spectra. (4) A spectral peak in the vertical velocity near the ground commensurate with the trunk diameter emerged at a moderate element Reynolds number consistent with Strouhal instabilities describing wake production.

1. Introduction

Interest in land vegetation–atmosphere scalar, energy and momentum exchange are now motivating theoretical and experimental studies on the structure of turbulence within the canopy sublayer (Baldocchi et al., 2000; IPCC, 2001), hereafter referred to as the CSL. In part, this interest stems from the recognition that at short time scales (e.g. seconds), most of the energy, gas and particle exchange between the atmosphere and the ecosystem takes place through turbulent motions that appear coherent and exhibit predictable statistical attributes. Hence, it comes as no surprise that turbulent flows inside forest canopies have received significant attention over the last four decades whether be it using field measurements (e.g. Allen, 1968; Cionco, 1972; Baldocchi and Meyers, 1988a,b; Amiro, 1990; Lee and Black, 1993a,b, Kruijt et al., 2000), wind tunnel and flume studies (e.g. Raupach et al., 1986; Finnigan and Shaw, 2000; Poggi et al., 2004a,b), theoretical models based on Eulerian closure principles and Lagrangian approaches (e.g. Shaw, 1977; Wilson and Shaw, 1977; Raupach and Thom, 1981; Kaimal and Finnigan, 1994; Raupach et al., 1996; Massman and Weil, 1999; Finnigan, 2000; Siqueira et al., 2000; Harman and Finnigan, 2007), and now with increased computational capacity, large-eddy simulations (e.g. Dwyer et al., 1997; Su et al., 2000; Albertson et al., 2001).

Finnigan's (2000) annual review summed up pending problems that must be confronted in the CSL, and they partly include diabatic effects and 'across-scale' turbulent energy cascade with possible modulations by wake generation for planar homogeneous CSL flows and the role of inhomogeneities such flows near forest edges or on complex terrain. Moreover, the past decade witnessed a proliferation of carbon and water cycling budgets that are clearly pointing out to the significance of forest soils and the understory in this exchange, particularly in forests with open canopies (Baldocchi and Vogel, 1996; Black et al., 1996; Law et al., 2001; Launiainen et al., 2005). There

*Corresponding author.
e-mail: samuli.launiainen@helsinki.fi
DOI: 10.1111/j.1600-0889.2007.00313.x

are also practical needs for progressing on all these problems, for instance, when interpreting variability in turbulent fluxes in relation to variability in material sources and sinks within ecosystems. Footprint estimates are known to be sensitive to the vertical distribution of sources and sinks from the ground to the canopy top and to the residence time of air parcels within the foliage (Hsieh et al., 2003; Markkanen et al., 2003; Strong et al., 2004). More realistic footprint estimations require improved description of canopy turbulence, yet the nocturnal properties of CSL turbulence characteristics, especially in the subcanopy pose unique challenges (Lee, 2000; Mahrt et al., 2000). Increasing atmospheric stability is known to suppress the scale of turbulent motion and reduce its transport efficiency. However, describing these reductions inside the canopy do not lend themselves to the 'niceties' of Monin–Obukhov similarity (e.g. Foken, 2006) as shown by a number of studies (Mahrt et al., 2000; Lee and Mahrt, 2005). According to Lee and Mahrt (2005), daytime subcanopy turbulence can be generated more by local buoyancy than downward transport of turbulence from above the canopy. On the other hand, strongly stable stratification above the forest floor during nighttime may cause decoupling of the flow in the subcanopy from the flow above. This situation promotes nocturnal drainage flows, which remains a 'thorny' issue in interpreting nocturnal CO_2 fluxes collected above the canopy and linking them to long-term ecosystem carbon sequestration (Aubinet et al., 2003; Feigenwinter et al., 2004; Staebler and Fitzjarrald, 2004; Yi et al., 2005). Despite its importance, only few previous studies have considered the turbulence properties in the lowest 20% of the canopy (Lee and Black, 1993a,b; Baldocchi and Hutchison, 1988; Baldocchi and Meyers, 1988a,b) and likewise for studies considering the effect of atmospheric stability within the canopy (Shaw et al., 1988; Leclerc et al., 1990, 1991; Brunet and Irvine, 2000; Kruijt et al., 2000; Villani et al., 2003).

Motivated by those data needs, we describe the turbulence statistics inside and above a Scots pine forest measured during an intensive field campaign in the summer of 2005 (Launiainen et al., 2006; Pumpanen et al., 2006). The main aims are to explore: (1) diabatic effects on the bulk flow properties as well as higher-order statistics pertinent to closure modelling, Lagrangian dispersion studies, and the ejection-sweep cycle and (2) the integral time scale statistics along with modulations of the spectra by spectral short-circuiting, wake production, and diabatic effects. The Hyytiälä SMEAR II-site is ideal to address these objectives because of the availability of long-term record of gas and particle exchange measured over the last decade (Vesala et al., 1998; Suni et al., 2003) as well as turbulence properties in the upper trunk-space and above the forest (Rannik, 1998; Rannik et al., 2003).

Throughout this paper, we use the following nomenclature: The overstory canopy (or canopy crown) refers to the needle layer. Below that, a relatively open trunk-space (or subcanopy) exists where the stems and only some dead branches impose drag on the flow. Forest floor refers to the lowermost layer above the ground including the low understory.

2. Materials and methods

2.1. Site description

The SMEAR II station is located in a Scots pine stand (*Pinus sylvestris* L.) sown in 1962 next to the Hyytiälä forest station of the University of Helsinki in southern Finland (61°51′N, 24°17′E, 181 m above sea level). The all-sided leaf area index (LAI) is 7 m^2 m^{-2} concentrating on the upper part (7–15 m above the surface) of the canopy (Fig. 1), and the tree density 1100–1200 ha^{-1} (Vesala et al., 2005). Thus, the average distance between the trunks is ∼3 m. The mean tree height (h_c) is 15 m and the mean diameter at breast height 16 cm. According to the Cajander site class system (Cajander, 1909), the stand is of medium fertility and has annual wood increment 8 m^3 ha^{-1} yr^{-1}. The forest is half way through the rotation time for this type of stand and the regeneration has been performed using standard silvicultural guidelines (Peltola, 2001). Thus, the stand structure is rather characteristic for a managed pine forest. The forest floor vegetation is relatively low (mean height ∼20–30 cm) and is dominated by dwarf shrubs, mainly lingonberry (*Vaccinium vitis-idaea*) and blueberry (*V. myrtillus*), and mosses (Kolari et al., 2006).

According to Rannik et al. (2003), the displacement height (d) and roughness length (z_{0m}) for momentum are 0.78 and 0.062 h_c, respectively. The site is subject to moderate height variation. Rannik (1998) has studied the above canopy flow statistics and flux-gradient similarity theory above the stand and these are not repeated here.

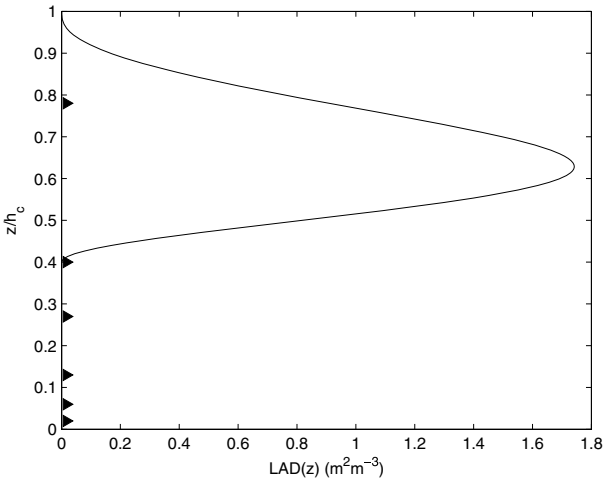

Fig. 1. Vertical profile of the all-sided leaf (i.e. needle) area density (LAD) of the Scots pine forest. Here z/h_c is the height above ground normalized by the canopy height h_c. The triangles on the left y-axis illustrate the measurement levels inside the canopy (Table 1).

Table 1. Measurement heights and measurement devices

Height above ground (m)	Relative height z/h_c	Sonic	Sonic path length (cm)	Measurement frequency	Gas-analyser
22.0	1.47	Solent Research[a] HS 1199	15.0	10.41	LI-6262[c]
11.7	0.78	Solent Research[a] 1012RS	15.0	10.41	LI-6262[c]
6	0.4	Metek[b] USA-1	17.5	10.0	
4	0.27	Metek[b] USA-1	17.5	10.0	
2	0.13	Metek[b] USA-1	17.5	10.0	LI-7500[c]
0.95	0.06	Metek[b] USA-1	17.5	10.0	LI-7500[c]
0.25	0.02	Solent Research[a] HS 1199	15.0	20.0	

[a]Gill Ltd, Lymington, Hampshire, England, [b]Metek GmbH, Elmshorn, Germany, [c]Li-Cor Inc., Lincoln, NE, USA.

2.2. Measurements of fluxes and turbulence statistics

A field campaign was carried out from 27 June to 15 July 2005 at the site. During the period, turbulence properties and fluxes were measured by eddy covariance method (EC) concentrated at five heights below the overstory canopy (0.25, 0.95, 2.0, 4.0 and 6.0 m), and at one level both within (11.7 m) and above the canopy crown (22.0 m). The measurement heights corresponding to the mean canopy height (h_c) are listed in Table 1 and Fig. 1. In subcanopy, the 3-D sonic anemometers were installed (details in Table 1) on a 7 m tall mast (diameter 75 mm) using 58 cm horizontal booms (diameter 40 mm). Exception of this was the sonic closest to the ground, which was located 3 m NW from the mast to minimize the flow distortion effects by the mast base. The sonics were aligned in the vertical with an accuracy of $<0.5^\circ$ using a level and inclinometers connected to sonics at 4 and 6 m heights. The mast was secured with support wires at two levels to increase rigidity after installation. Use of a delicate mast minimizes the flow distortion, though likely to be small (and similar to a wake behind a trunk) due to low wind velocities inside the stand. The distance to the nearest trees was 2–3 m depending on the direction. All the sonics were sampled with the same computer connected to the central timing system of the measurement station for synchronization.

Measurements within and above the overstory canopy were collected at a larger tower located 25 m SW (220°) from the below canopy mast. At 11.7 m height, an anemometer was installed on the north face of the measurement tower on a 2.5 m horizontal boom less than a meter away from the nearest branch. The sonic above the stand (22.0 m) was operating at the top of the tower. Details of all the measurement setups are listed in Table 1. The raw data from all sonics were stored onto hard drives for post-processing. Loescher et al. (2005) provide a comparison of different sonic anemometer types including the ones used in this experiment. According to their results, the vertical wind variance measured by USA-1 sonic was approximately 10% less than what was measured by the Gill R3 but the situation was opposite for horizontal wind variance. Although the value may seem large, these differences are small compared to the vertical differences expected between the trunk-space and the canopy crown flow statistics. Because of minor in-homogeneity in the topography and vegetation at the site (Rannik, 1998), some care must be exercised when separating vertical variability from possible horizontal variation when turbulence profiles are measured at two different locations.

There is some degree of uncertainty over the appropriate coordinate system and detrending of the turbulent time series when performing of flux calculations and boundary-layer analyses (Finnigan et al., 2003; Finnigan, 2004). However, we calculated half-hourly mean fluxes and statistics using common methods (Euroflux-methodology, Aubinet et al., 2000). First, we applied a 3-D flow distortion correction algorithm provided by the manufacturer for all raw wind velocities sampled by USA-1 sonics (Table 1), removed spurious spikes from the data and applied a 2-D coordinate rotation for the wind components. In this rotation, the x-axis is forced along the mean wind direction and the mean vertical velocity ($\overline{w}$) is forced to zero (Kaimal and Finnigan, 1994). After coordinate rotation, u represents the streamwise, v the lateral and w the vertical component. We calculated the fluxes and statistics consistently at all levels using linear detrending and chose the normal sign convention with negative fluxes indicating downward transport of the quantity. We omitted the wind directions possibly influenced by the tower structures from the further analysis.

2.3. Auxiliary measurements

We measured temperature, humidity and CO_2 at several levels between 4.2 and 67 m at a high mast, about 60 m west from the subcanopy tower (Vesala et al., 1998) and used temperature data in the analysis. We monitored the present weather conditions using FD12P Weather Sensor (Vaisala Oyj, Helsinki, Finland) and removed rainy periods from the further analysis. We also conducted eddy-covariance measurements of CO_2 and H_2O at two levels in the trunk-space (0.95 and 2.0 m), within the crown (11.7 m) and above the canopy (22.0 m) connecting the analogue signals from the gas-analysers to the respective sonics for synchronization (Table 1). However, we do not report these flux measurements in this study.

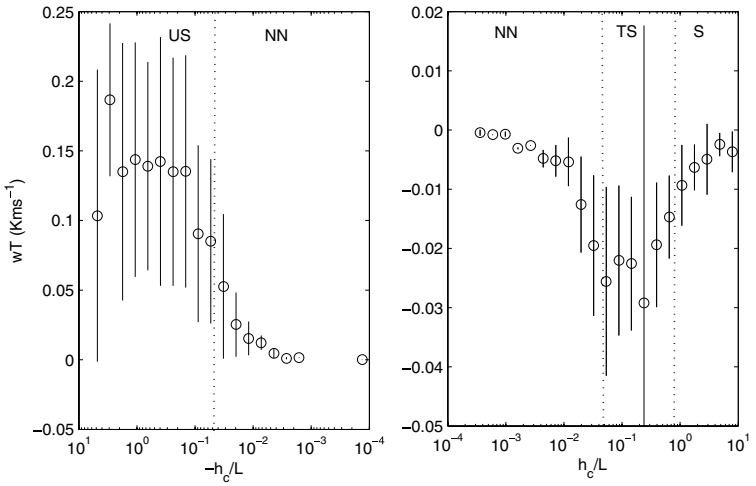

Fig. 2. Kinematic heat flux (wT) as a function of stability (h_c/L). Shown are mean $\pm$ *SD*. Stability regimes are defined as: unstable (US), near-neutral (NN), transition regime (TS) and very stable (S).

To obtain the vertical distribution of foliage, we converted the needle dry mass vertical profile (Ilvesniemi and Liu, 2001) to vertical profile of leaf (i.e. needle) area density (LAD) (Fig. 1). In this conversion, we used data on spesific needle area (SNA, i.e. total needle area per dry weight) and STAR (spherical average of shoot silhouette to total needle surface area ratio) change along the profile of available light inside a Scots pine canopy (Stenberg et al., 2001) with a simple light penetration model based on homogeneous canopy and spherical distribution for element orientation.

2.4. Data presentation and normalizing variables

To explore the diabatic effects on the flow statistics, vertical profiles of different turbulence statistics are classified into four different stability regimes. We use the canopy height (h_c) as the primary length scale (Raupach, 1989) and the Obukhov length (L) derived from above-canopy measurements as the stability parameter. We follow Mahrt et al. (1998) and define the different stability regimes based on the behaviour of buoyancy heat flux ($\overline{w'T'}$) above the canopy as a function of stability (Fig. 2): The near-neutral (NN) regime corresponds to h_c/L interval in which $\overline{w'T'}$ remains close to zero. In the transition stable regime (TS) the (downward) heat flux decreases rapidly as a function of h_c/L due to decreasing amplitude of the vertical fluctuations associated with stability constraints, while in very stable regime (S) $\overline{w'T'}$ is small but continues to decrease slowly with increasing stability. In the unstable regime (US) the heat flux is large positive. This approach suffers from self-correlation ($\overline{w'T'}$ is included in both axis of Fig. 2.) but provided the same results as gradient-Richardson number based approach (not shown) that is an independent measure of the stratification. The different stability regimes (Fig. 2.) used in this study are: (1) unstable (US) $h_c/L < -0.05$, (2) near-neutral (NN) $\mid h_c/L \mid \leq 0.05$, (3) transition stable regime (TS) $0.05 < h_c/L < 0.8$ and (4) very stable (S) $h_c/L \geq 0.8$. The number of half-hour observations in each regime was 269 (US), 123 (NN), 152 (TS) and 63 (S). The friction velocity (u_*), used to normalize the turbulence statistics, was derived from the momentum flux measurements at 22.0 m height as $u_* = (\overline{u'w'}^2 + \overline{v'w'}^2)^{1/4}$.

We plot the profiles against dimensionless height z/h_c and show, if nothing else stated, the median values of each parameter with lower and upper bars corresponding to 25 and 75% quantiles, respectively. We chose this approach to represent typical values given expected departures from Gaussianity. Note that the wideness of distribution shown includes not only the random errors but also changes in synoptic conditions within the defined stability regimes. There are both practical and theoretical justifications for presenting the data using such ensemble-averages here. On the theoretical side, turbulent canopy flow models (e.g. Raupach and Thom, 1981; Kaimal and Finnigan, 1994; Finnigan, 2000) are based on volume (or spatially) averaged statistics. Hence, single point statistics may only be interpreted as 'spatial averages' after ensemble averaging over a wide range of wind directions assuming the Ergodic hypothesis remains valid (e.g. Katul et al., 2004). On the practical side, such ensemble averaging reduces the random error component.

3. Results and discussion

To address the two study objectives, vertical variations of the bulk flow statistics, including second-order statistics most relevant to standard higher order closure modelling, are first presented and discussed in the context of how diabatic effects alter their canonical shapes. Next, higher-order statistics (including univariate skewness and flatness factors), known to be indicators of key attributes of the ejection-sweep cycle, are discussed. Finally, the integral time scale statistics along with modulations of the energy spectra by short-circuiting of the energy cascade, wake production, and diabatic effects inside the canopy are presented.

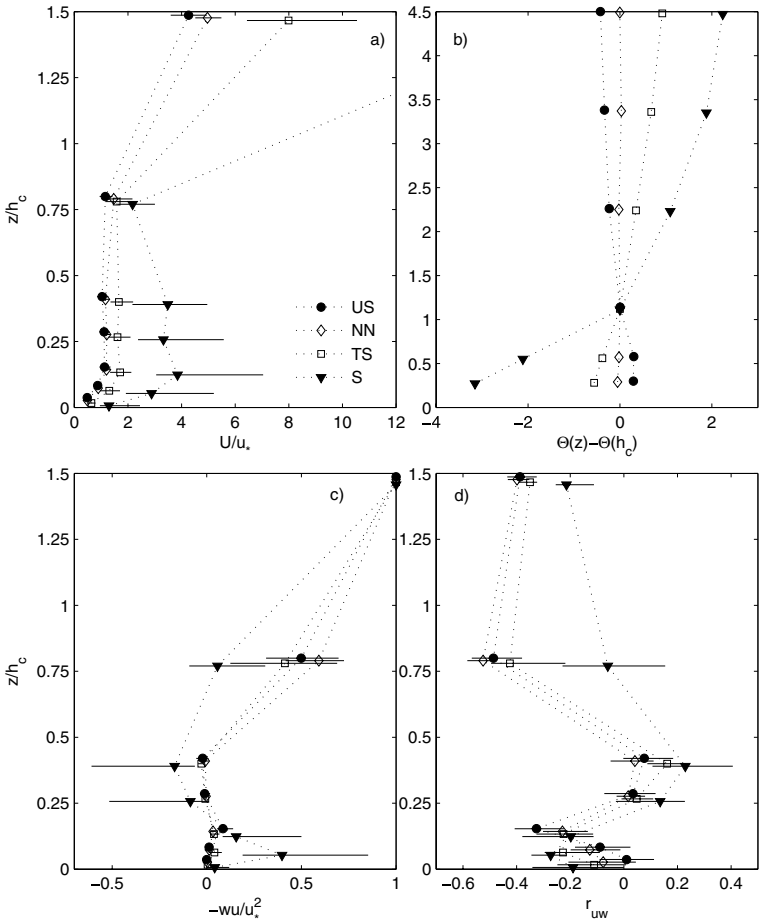

Fig. 3. Mean wind speed (U/u_*) profile (a), potential temperature profiles (b), normalized momentum flux (c) and correlation coefficient r_{uw} (d) profiles in different stability regimes: Unstable (US), near-neutral (NN), transition stability (TS) and very stable (S). Different symbols show the median values and solid lines represent 25th / 75th percentiles. For clarity, the values are slightly shifted in vertical. In panel (a) U/u_* at the highest level during S is not shown. The value is 18.2.

3.1. Vertical profiles of turbulence statistics

3.1.1. Mean wind speed, momentum flux and standard deviations. The mean wind speed (U) exhibits strong shear just above and in the upper part of the canopy. In contrast, normalized U was rather constant and exhibited a weak secondary maximum in the lower trunk-space within the subcanopy (Fig. 3a). Close the forest floor ($z/h_c < 0.2$) the wind speed profile recovered an approximately logarithmic shape, suggestive of an emergence of a new boundary layer despite the weak momentum flux towards that boundary. Throughout, the normalized wind speed within the canopy increased markedly as diabatic effects progressively changed from unstable to stable conditions. In fact, the most notable feature is a more pronounced secondary maximum for stable conditions resembling those reported inside forest canopies by others (e.g. Shaw, 1977).

In Fig. 3b, the mean potential temperature profiles across different stability regimes are shown. Particularly during stable nights (S), the subcanopy inversion was strong: The temperature in the trunk-space was on average over 3 K lower than at the canopy top. The temperature difference between the trunk-space and the canopy top was much smaller during near-neutral and unstable stratification. The observed temperature profiles indicate that the diabatic stability in trunk-space follows the diabatic stability of the surface layer, which is typical in open canopied forests. Part of the strong subcanopy inversion during very stable stratification above the canopy may be a result of placing the temperature sensors on a mast located in a small gap in the canopy. However, the virtual temperature profile measured by USA-1 sonics (Table 1), although not accurate, showed consistent behaviour at different location. Hence, the relatively open pine canopy at the site differs markedly from dense canopies, in which the temperature structure can be opposite to the overlying surface layer (e.g. Bosveld et al., 1999; Krujt et al., 2000).

The normalized momentum flux ($-\overline{u'w'}/u_*^2$) decreased rapidly in the canopy crown due to momentum absorption by the foliage and reached a level close to zero below the main canopy (Fig. 3c). Similar to observations by Lee and Black (1993a) in a Douglas-fir forest, upward momentum fluxes were observed above the secondary wind maximum (Fig. 3a), especially during the very stable case. The correlation coefficient, $r_{uw} = \overline{u'w'}/\sigma_u\sigma_w$, is a measure of momentum transport efficiency (Fig. 3d). Above the canopy r_{uw} was roughly -0.4 in all stability regimes showing some organization of flow except

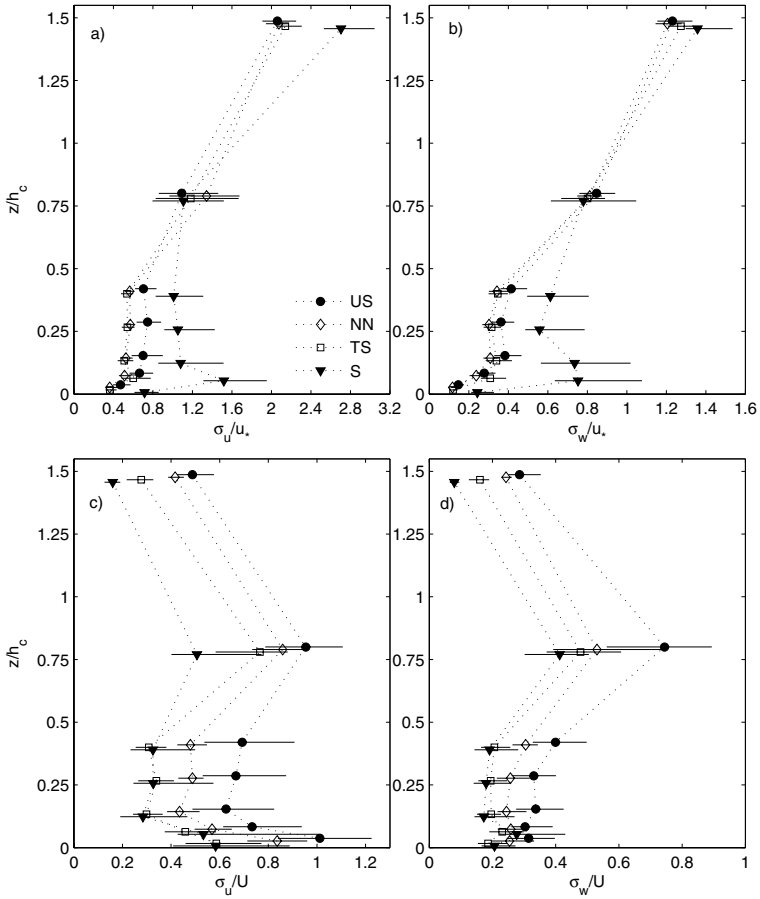

Fig. 4. Normalized standard deviations (σ_i/u_*) of u (a) and w (b) as well as streamwise (c) and vertical (d) turbulence intensities.

in very stable regime when it decreased to around -0.21. In the canopy crown, r_{uw} increased and ranged from -0.4 to -0.5 except in very stable case (~ -0.06). In the upper trunk-space, r_{uw} became positive (most positive in TS and S) at heights above the secondary maximum. Close the forest floor r_{uw} was between -0.3 and $+0.05$ and the scatter in the data is too large for more detailed analysis. In US, NN and TS regimes r_{uw} was similar to values reported in Raupach et al. (1996).

The u_* -normalized standard deviations of u, v and w (σ_u, σ_v and σ_w, respectively) varied significantly as a function of height (Fig. 4a and b). Above the canopy σ_u/u_* ranged from 2.06 (US and NN) to 2.93 (S) while σ_w/u_* was 1.21 (NN) and 1.38 (S). Above the forest and inside the overstory both components decreased but were roughly constant with height in the trunk-space. During US to TS stratification, σ_u/u_* and σ_w/u_* ranged from 0.5 to 0.8 and from 0.3 to 0.4, respectively. The very stable regime differs significantly from the other stabilities in the trunk-space (Fig. 4a and b): σ_u/u_* and σ_w/u_* were much larger, from $\sim$1.0 to 1.5 and from 0.55 to 0.75, respectively. The smallest values appeared at all levels when stratification was close to neutral, qualitatively as predicted by standard surface layer relationships (Kaimal and Finnigan, 1994; Zhang et al., 2001). However, the similarity theory was in quantitative agreement only above the canopy and stronger increase in σ_u/u_* and σ_w/u_* with increasing/decreasing stability was observed in the subcanopy and above the understory layer (data not shown). As Mölder et al. (2004), we found that the influence of stability on σ_u/u_* and σ_w/u_* increased towards the forest floor. The observed values of the normalized standard deviations are in agreement with previous studies (Amiro, 1990; Green et al., 1995; Raupach et al., 1996; Novak et al., 2000; Mölder et al., 2004). Particularly the large values of σ_u/u_* in the trunk-space indicate intense turbulent motion inside the stand that is inactive in the sense of momentum transport (Finnigan, 2000). Hence, the emerging picture from this analysis with regards to the trunk space is the following: The dimensionless turbulent kinetic energy (TKE) in the trunk space appears large primarily due to the large σ_u/u_*, the intense TKE is inactive and does not contribute to momentum fluxes. The origin of this inactive eddy motion is likely to be the very upper layers of the canopy where the flow instabilities are produced by the strong shear (Fig. 3a), and these eddies then loose their momentum transporting efficiency to the canopy drag elements to become inactive within the deeper trunk space.

The turbulence intensity (local σ_i divided by local U) is a measure of the gustiness of the wind field. We observed the largest intensities of horizontal turbulence in the canopy crown

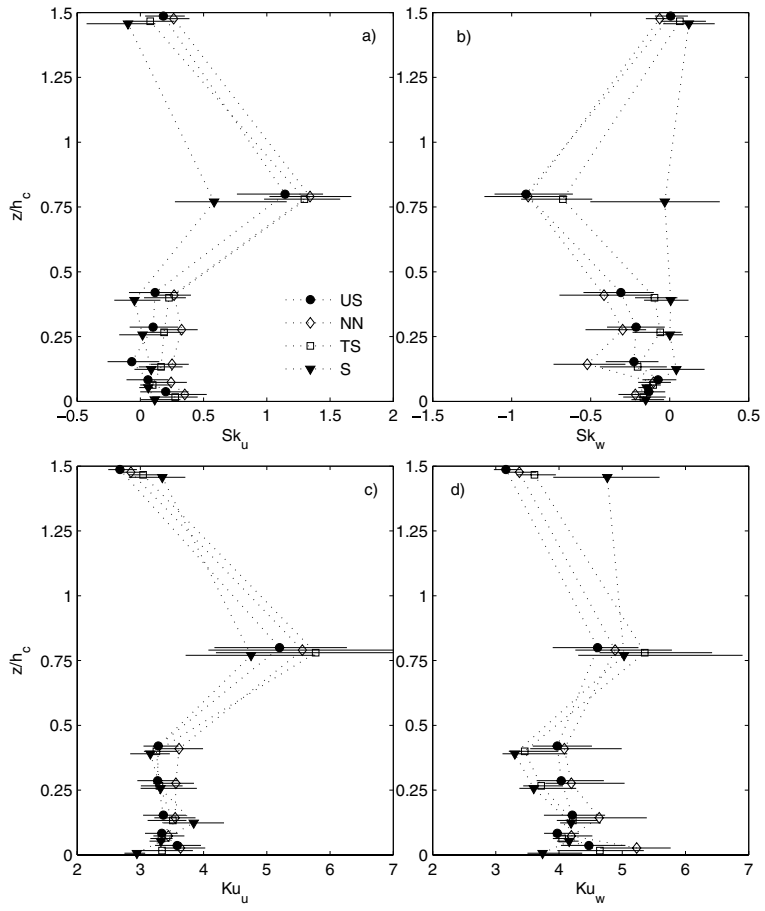

Fig. 5. Skewness (Sk) (a and b) and kurtosis (Ku) (c and d) of streamwise (u) and vertical (w) component.

and closest to the ground where σ_u was of the same order as U during unstable stratification (Fig. 4c). Turbulence intensities were smaller in the open trunk-space where the drag against the flow is weaker and, therefore, the local production of turbulence is weak. Figure 4d shows that throughout the stand σ_w/U was smaller than σ_u/U, especially close to the ground where the vicinity of the ground surface suppresses the vertical eddies. We do not show the lateral component (v) here but it resembled the streamwise (u) component. Baldocchi and Meyers (1988a) and Lee and Black (1993a) have reported similar behaviour in deciduous and in Douglas-fir forests, respectively. In general, increasing stability decreased the turbulence intensities while the buoyant production of turbulence above the forest floor may be significant during unstable daytime conditions (Fig. 4c and d).

3.1.2. Skewness and kurtosis. Over the past decade, a number of attempts have been made to link the asymmetry in the probability density function (pdf) to higher-order closure modeling with particular attention paid to the flux-transport term (e.g. Katul et al., 1997b; Poggi et al., 2004b; Cava et al., 2006; Katul et al., 2006). These attempts were stimulated by the fact that the degree of asymmetry in the probability density function is an elementary indicator of the strength of the ejection-sweep cycle, though how diabatic effects may modify this asymmetry remains to be explored for the CSL. The influence of diabatic effects on the asymmetry of the pdf in the atmospheric surface layer is better understood as summarized by Chu et al. (1996). The variation in the skewness of u and w ($Sk_i = \overline{u_i'^3}/\sigma_i^3$) are shown across the four stability classes in Fig. 5. Above the canopy Sk_u and Sk_w (Fig. 5a and b) were close to the Gaussian value (zero) but in the trunk-space u was positively (from 0 to 0.3) and w negatively (from 0 to -0.5) skewed as found by several authors in the field (Baldocchi and Meyers, 1988a; Lee and Black, 1993a; Katul and Albertson, 1998; Katul and Chang, 1999; Finnigan, 2000; Novak et al., 2000; Villani et al., 2003) and in a flume for dense rods (Poggi et al., 2004a). This behaviour is consistent with the importance of energetic downward moving gusts penetrating the canopy and reaching the forest floor (Raupach et al., 1996; Finnigan, 2000). In the canopy crown, Sk_u and Sk_w were at their largest (absolute values), from 0.5 to 1.3 and from 0 to -0.9, respectively, again in line with previous studies. Sk_v (not shown) was negative inside the canopy crown (from -0.2 to -0.6).

The kurtosis ($Ku_i = \overline{u_i'^4}/\sigma_i^4$) is often used as a measure of intermittency (beyond Gaussianity) of turbulence (Fig. 5c and d),

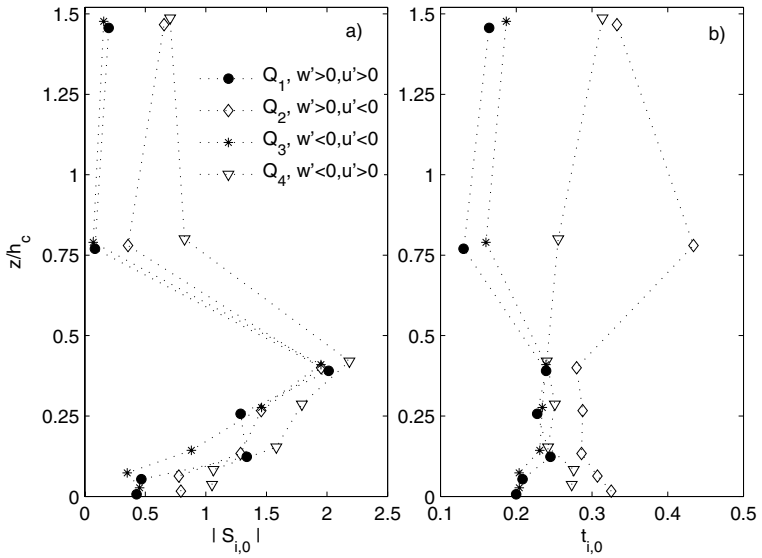

Fig. 6. Contribution of different quadrants to momentum transport (eq. 1) during near-neutral stratification with hole size zero (a) and corresponding time fractions (eq. 2) (b). Quadrants 2 and 4 (ejections and sweeps) transport momentum downwards and quadrants 1 and 3 upwards. Number of 30 min runs averaged is 123.

with high kurtosis suggestive of 'on-off' processes. Ku_u was close to the Gaussian value of 3 above the canopy, slightly larger in the trunk-space (∼3.5) and significantly larger in the canopy crown (from 5 to 6). Ku_v (not shown) behaved similarly. Ku_w was approximately 3.5 above the canopy and ranged from 3.5 to 5.5 in trunk-space with increasing values with decreasing height. Baldocchi and Meyers (1988a) have reported similar behaviour in deciduous and Amiro and Davis (1988) in spruce and Lee and Black (1993a) in Douglas-fir forests. The largest values of Ku_w appear in the canopy crown and closest to the surface. Interestingly, Poggi et al. (2004a) also showed increased Ku_u and Ku_w with increased canopy density inside a canopy composed of cylindrical rods within a water channel, with maximum Ku_u reaching 4.5 and maximum Ku_w reaching 5.5 as well. The Sk_u and Ku_u were rather insensitive to stability changes although Sk_u was closest to zero during very stable stratification, particularly in the canopy crown. Sk_w was closest to the Gaussian value during stable and furthest away during near-neutral stratification at all levels (Fig. 5b). We observed the same in Ku_w in the trunk-space but found above the canopy the most Gaussian behaviour during unstable conditions (Fig. 5d).

3.1.3. Conditional analysis of the momentum flux. Another quantitative indicator of the strength of the ejection-sweep cycle in momentum and scalar transfer is via conditional sampling (Baldocchi and Meyers, 1988a; Bergström and Högström, 1989; Poggi et al., 2004a; Cava et al., 2006; Katul et al., 2006). In brief, the $u'w'$—terms are divided into four quadrants depending on the sign of the instantaneous fluctuations and are labeled as: (1) outward interaction ($u'>0$, $w'>0$), (2) ejection ($u'<0$, $w'>0$), (3) inward interaction ($u'<0$, $w'<0$ and (4) sweep ($u'>0$, $w'<0$). As a consequence, quadrants 2 and 4 (ejections and sweeps) contribute to downward and quadrants 1 and 3 to upward flux of horizontal momentum. A stress fraction ($S_{i,H}$) and time fraction ($t_{i,H}$) are defined, respectively as

$$S_{i,H} = \frac{1}{|\overline{u'w'}|}\frac{1}{T}\int_0^T u'(t)w'(t)I_{i,H}\mathrm{d}t, \tag{1}$$

$$t_{i,H} = \frac{1}{T}\int_0^T I_{i,H}\mathrm{d}t, \tag{2}$$

where T is the averaging period, $I_{i,H}$ is a conditioning function which equals to one if the point $[u'(t),w'(t)]$ is located in the ith quadrant and $|u'(t)w'(t)|/|\overline{u'w'}| \geq H$ and zero otherwise. The dimensionless excursion parameter (H) is called hole size and, thus, $H = 0$ includes all events. Details of the quadrant-hole method can be found, for example, in Antonia (1981).

The contribution from different quadrants to the total momentum flux (at $H = 0$) and the corresponding time fractions varied significantly with height as shown in Fig. 6 where the median values of near-neutral periods are shown. Above the canopy, sweeps and ejections dominated the momentum transport ($|S|$∼0.7, Fig. 6a). Both occurred ∼30% of the time (Fig. 6b) consistent with numerous studies reviewed in Katul et al. (1997b; see their Table 2). Inside the canopy crown, the contribution from intermittent sweeps increased: ejections, although appeared about twice as frequently ($t_{2,0}$ ∼45%), transported more than two times less momentum($|S_{2,0}|$∼0.4). The contribution from the interactive quadrants was minor and they both occurred only during ∼15% of time. In upper trunk-space (z/h_c∼0.4), the situation was different with all quadrants having comparable magnitudes ($|S|$∼1.8 to 2.2) and time fractions with small dominance of sweeps. The stress fractions larger than unity suggest, as stated by Baldocchi and Meyers (1988a), that the momentum flux is composed of relatively small sum of large contributions of all four quadrants and are according to them associated with tall forests or orchards and aeroelastic canopies. Closer to the forest floor, the sweeps and ejections retained dominance and the stress fractions were

Table 2. Parameter values used to fit Massman and Weil (1999) model to the near-neutral observations

Parameter	Value	Description
$C_d(z)$	0.15	Drag coefficient, constant with height
LAI	3.5	One-sided leaf area
α	0.06	Empirical constant for within canopy length scale (Wilson and Shaw, 1977)
P_m	1.0	Sheltering factor
σ_u/u_*	2.08	Upper boundary conditions (Fig. 4)
σ_v/u_*	1.65	
σ_w/u_*	1.21	

reduced. Baldocchi and Meyers (1988a) interpret this as a result of smaller scale turbulence. Quadrant-profiles and their relative importance did not show any significant dependency on the stratification suggestive that diabatic effects do not alter qualitatively the role of sweeping motion in transporting momentum.

The sweep-to-ejection -ratio, $S_{4,0}/S_{2,0}$, ranged from 1.05 above the canopy (i.e. almost in balance) to 2.3 inside the canopy crown. These results are similar to observations by Baldocchi and Meyers (1988a) in deciduous forest as well as to results in Green et al. (1995) in spruce and Lee and Black (1993a) in Douglas-fir forests, Katul and Albertson (1998) in a pine forest, and to Poggi et al. (2004a) for the flume experiments.

3.1.5. Diabatic effects on the statistical moments and comparison to other studies. Our observations of the above and within the canopy mean velocity profiles agree with the inflectional instability and the analogy to a plane-mixing layer flow (Raupach et al., 1996) except for stable conditions. Brunet and Irvine (2000) studied how the streamwise spacing of the coherent eddy structures, that are the dominant features in canopy turbulence, depends on stability. They found that in stable conditions, the streamwise separation decreases because of the inhibition of turbulence by the stability forces, but observed no change in unstable conditions relative to neutral stratification. They hypothesize that stability forces do not act directly on the eddy length scales but primarily through modifying the mean wind profile, and, thus, on the shear length scale ($U(h_c)$ $[\mathrm{d}U(h_c)/\mathrm{d}z]^{-1}$) regulating the rate of generation of the active eddies as well as their characteristic length scales. These in turn strongly affect the flow inside the vegetation.

The shear stress attenuated faster and the correlation coefficient (r_{uw}) became smaller within the canopy with increasing stability (Fig. 3c and d). Also Shaw et al. (1988) observed a strong reduction in the momentum penetration into a deciduous forest canopy during evening, when the thermal structure of the surface layer changed from unstable to stable. They found that the momentum penetration depth in stable conditions ($0.4 < h_c/L < 0.8$) decreased relative to near-neutral conditions. They concluded that this effect was similar in magnitude as a transition from a fully leafed (LAI $\sim$ 4.9) canopy to almost defoliated one (LAI $\sim$0.3). Studying a tropical rain forest canopy, Kruijt et al. (2000) found similar stability dependency of the shear stress. The vertical profile of the relationship between the mean wind speed (U) and the shear stress (u_*) depends also on stability (Fig. 3a), especially in very stable regime. Kruijt et al. (2000) observed that the ratio U/u_* increased in a rain forest subcanopy and the secondary wind maximum became more distinct with increasing departures from neutral stability. Our results agree with this in stable conditions; however, the wind profiles measured here in the unstable regime did not markedly differ from neutral case. Baldocchi and Meyers (1988a) found that U/u_* increased in a deciduous forest subcanopy during nighttime when compared to slightly unstable daytime conditions and conclude this to be related to the stability of the nocturnal boundary layer, which acts to dampen the turbulence. We did not study the reasons for the observed secondary wind maximum in detail, but theoretically, it can occur in horizontally homogenous canopy when the net convergence of shear stress ($\overline{u'w'}$) transport exceeds the pressure—velocity gradient correlation (Shaw, 1977). Considering the small heterogeneities in vegetation and slightly undulating topography at the site, the likely reasons may also include a horizontal pressure gradient and drainage flows. Recently, Harman and Finnigan (2007) proposed a theory for the flow in the canopy and roughness sublayer, in which the displacement height and roughness length are significantly dependent on surface layer stability, and were able to resolve large part of the variation of U/u_* with stability. They found that the roughness sublayer (RSL) mitigates the influence of the boundary layer stability to the wind profile but RSL influence is not strong enough to remove or reverse the effect of the surface layer stability.

Leclerc et al. (1991) examined the influence of stability on the third moments inside deciduous forest and concluded that the buoyancy significantly affects the magnitude of gusts inside tall vegetation. They found that the velocity distributions were most skewed in neutral conditions and a departure from the neutral state significantly decreased the skewness (Sk) making the distributions more Gaussian. According to them, the large eddies developing in the convective boundary layer are weaker but more long-lived than in neutral conditions and, consequently, the velocity Sk and kurtosis (Ku) become smaller. On the other hand, the stability damps turbulence in stable conditions; the coherent structures are smaller and not as efficient in penetrating the canopy leading, again, to smaller Sk. We found the same

behaviour that Sk_u and Sk_w decreased with increasing stability / instability, although the differences between the stability regimes were small (Fig. 5). In very stable conditions, the weak and intermittent nature of turbulence was distinct: Ku_w was large above the canopy and Sk_w slightly positive throughout the stand. Leclerc et al. (1991) relate this behaviour in mid-canopy, during very stable conditions, to positive heat flux (rising thermals) found in this region. The sensible heat flux (H) profile (not shown), indeed, indicated a weak upward (counter-gradient) heat flux in the trunk-space, that according to Leclerc et al. (1991) may result from the intermittent turbulence. In stable stratification, a fluid parcel forced downwards is warmer than its surroundings in the lower canopy. Therefore, it experiences positive buoyancy and overshoots a short distance because of its momentum sinking then back to its original level. This would explain the positive heat flux observed in these regions. However, the observed H in trunk-space here was very small. Therefore, the relative uncertainty of its value and, more importantly, sign was too large to make any further conclusions. Also Kruijt et al. (2000) and Villani et al. (2003) found that the most non-Gaussian behaviour occurs for near-neutral conditions in a rain forest and a hardwood forest, respectively. Baldocchi and Meyers (1988a) divided the deciduous forest data into daytime and nighttime and found somewhat different results: in nighttime Sk_w and Ku_w were smaller in subcanopy but larger within the canopy crown, while there was no apparent change in Sk_u and Ku_u.

The turbulence intensities (Fig. 4c and d) decreased with stability as expected. In fact, Shaw et al. (1988) found that influence of thermal stratification on σ_w/U was larger than that of foliage density. The normalized standard deviations (Fig. 4a and b) depended also on the stability but the dependence was more complex. In unstable conditions there was more horizontal turbulence in trunk-space relative to the above canopy shear stress, which follows from local small-scale convection. In very stable stratification, the increase in σ_w/u_* and σ_u/u_* close the forest floor together with the stronger secondary wind maximum (Fig. 3a) suggests that there should be some local source of air movement in the trunk-space since the vertical transport is weak. However, we did not study this in detail. When the conditions above the canopy were very stable, Krujt et al. (2000) found markedly increased values of σ_w/u_* and σ_u/u_* in a rain forest subcanopy. A smaller increase was found during unstable stratifications. Although these resemble our results, it is likely that the processes responsible are partly different taking account the substantial differences in the canopy structure and in the thermal stratification of the canopy layer between a pine forest and a tropical rain forest.

3.1.6. Turbulent time scales. One popular 'measure' of the degree of organization in a stationary time series is the integral time scale, though other measures have also been proposed but not considered here (e.g. see Wesson et al., 2003 for a review). We calculated the Eulerian time scales of different variables (T_{Ei}) for each level integrating the single-point autocorrelation function (τ_i) to first $1/e$ ($\sim$0.37) crossing (Kaimal and Finnigan, 1994; Mölder et al., 2004). We derived the Lagrangian integral time scales from T_{Ei} using a relationship suggested in Raupach (1989)

$$T_L = \beta \frac{U}{\sigma_w} T_E, \tag{3}$$

where β is a constant of the order of unity (in this study $\beta = 1$) and U and σ_w are height-dependent local values. Equation (3) is derived starting from Taylor's (1921) kinematic theorem, an estimate of the Lagrangian diffusivity (K) based on a characteristic length (L_w) and characteristic velocity scale (σ_w), and the subsequent use of Taylor's frozen turbulence hypothesis to convert L_w to T_E so that

$$T_L = \frac{K}{\sigma_w^2} = \frac{(\beta L_w)\,\sigma_w}{\sigma_w^2} = \beta \frac{U}{\sigma_w} T_E. \tag{4}$$

The integral time scales (normalized here by u_*/h_c) varied with height and stability (Fig. 7). T_{Ew} (Fig. 7a) had maximum values in trunk-space and was shorter within and above the overstory canopy. T_{Eu} (Fig. 7b) was longest above the canopy and decreased rapidly at the canopy top having a minimum inside the canopy crown. In trunk-space, T_{Eu} increased again and was comparable to values observed above the canopy. Both time scales decreased rapidly close to the surface as suggested in Mölder et al. (2004). T_{Eu} and T_{Ew} decreased with increasing stability, consistent with reduction in eddy sizes with increased stability. The Lagrangian time scales T_{Lw} and T_{Lu} (Fig. 7c and d) showed the same behaviour with height as their Eulerian counterparts with maximum above the canopy and in trunk-space and minimum in the canopy crown. Lai et al. (2002) studied the stability dependence of T_{Lw} just above a Loblolly pine canopy and found that T_{Lw} decreased greatly with increasing stability (a reduction factor of 10 for 2 decades of h_c/L). They also provided a profile of T_{Lw} inside the canopy derived from T_{Ew} measurements, assuming $T_L \sim 4/3 T_E$, and found that T_L increased from the canopy top towards the subcanopy by roughly a factor of three. Their findings are similar to the results obtained in this study with an exception that they did not observe the decrease of T_L above the forest floor. The pine forest in Lai et al. (2002) was denser (projected LAI $\sim$3.5) and the onset of a local boundary layer near the ground may not have occurred. We note that the linear relationship between T_L and T_E in Lai et al. (2002) differs from equation (3). Its genesis is based on the relationship by Tennekes (1979) who showed that

$$T_L = \frac{2\sigma_w^2}{C_o \varepsilon}, \tag{5}$$

where C_o is the Kolmogorov constant for the Lagrangian structure function, and ε is the mean TKE dissipation rate. In a neutral surface layer, $\varepsilon = u_*^3/(k_v z)$, and hence

$$T_L = \frac{2\sigma_w^2}{C_o u_*^2}\left(\frac{k_v z}{u_*}\right) = \frac{2\sigma_w^2}{C_o u_*^2} T_E = \left(\frac{2\,A_w^2}{C_o}\right) T_E, \tag{6}$$

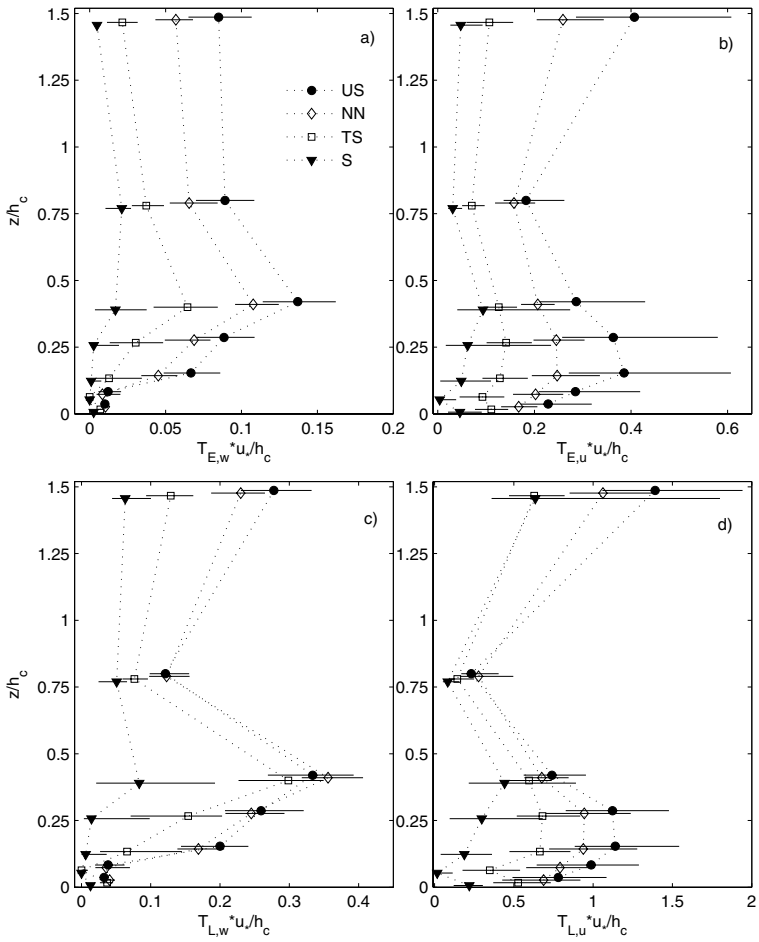

Fig. 7. Normalized Eulerian time scales of w (a) and u (b). Corresponding Lagrangian time scales (eq. 3) (c and d).

where k_v is the Von Karman constant, and $\sigma_w/u_* = A_w$ is a constant for the neutral atmospheric surface layer. There is considerable uncertainty around C_o(e.g. see Table 1 from Lien and D'Asaro, 2002), but all in all, the above expression predicts a linear relation between T_L and T_E with almost 1:1 correspondence when using $A_w = 1.25$ and $C_o = 3.125$. Hence, using the above interpretation, Fig. 7a and b may also be interpreted as alternative estimates to T_L.

Leuning (2000) included the impact of atmospheric stability on T_L by assuming that the standard Monin–Obukhov (M–O) similarity functions can be used within the roughness sublayer, when the stability parameter is defined as h_c/L. Using this approach, it was demonstrated that T_L had strong dependence on stability for $\mid h_c/L \mid < 0.2$ but was much less sensitive to further changes in stability. His values of T_L for strongly unstable ($h_c/L \sim -2$) and very stable ($h_c/L \sim 1$) stratification show an increase by a factor of 1.6 and a decrease by roughly a factor of 5 when compared to neutral values, respectively (Leuning, 2000, Fig. 1). The corresponding fractions above the canopy here were ∼1.3 in unstable and from 2 to 4 in very stable regime, and the relationship remained (at least qualitatively) similar all the way down to the forest floor. Figure 7 shows also how T_L in the very stable regime differs from the other stability regimes, which is contrary to Leuning (2000), who showed that the largest influence of atmospheric stability occurred at moderate deviations from near-neutral stratification. On the other hand, the findings here are consistent with observations reported in Lai et al. (2002).

Mölder et al. (2004) used same approach as Leuning (2000) and observed that under stable conditions the variations in T_E can be well described using the M–O similarity functions when neutral states were determined from data collected within a Scots pine stand. We carried out the same analysis here and found a similar result: in a fairly open pine canopy, the T_{Ew} followed reasonably well the M–O based similarity function (Leuning, 2000) for stable conditions at all heights from above the canopy down to forest floor (data not shown). Under unstable stratification, the overall fit to the theoretical curve was much worse and T_{Ew} actually decreased with increasing instability (when $h_c/L < -0.1$), entirely in agreement with Mölder et al. (2004).

According to our results, a T_L (u_*/h_c) ∼0.3 derived by assuming $T_L \sim 4/3T_E$ (Legg et al., 1986; Katul et al., 1997a), would be an overestimation of T_{Lw} throughout the stand (Fig. 7c)

during very stable conditions. In addition, independently of the stratification, T_{Lw} would be overestimated within the canopy crown and close to the ground surface, in line with Lai et al. (2002). Both they and Leuning (2000) showed that inclusion of stability dependence to T_L improves significantly the accuracy of inverse Lagrangian dispersion analysis they used to derive scalar source/sink distributions in plant canopies. Moreover, the flume experiments in Poggi et al. (2006) suggest that T_{Lw} (u_*/h_c) is of the order 0.1 with a reduction up to 0.05 midway in their dense canopy (composed of rods), consistent with the near-neutral runs shown in Fig. 7. The implications of a smaller T_{Lw} (u_*/h_c) than 0.3 are significant in Lagrangian stochastic modelling approaches (e.g. Rannik et al., 2003; Poggi et al., 2006). For example, in the standard Thomson (1987) model for the velocity excursions, the dispersion term is related to $\sqrt{C_o\varepsilon}$ and the drift term is partially impacted by $C_o\varepsilon$. Hence, an overestimate of T_{Lw} means an underestimate of $C_o\varepsilon = \frac{2\sigma_w^2}{T_L}$ and thereby makes both the drift and random components much smaller in those models.

Our results together with the findings of Mölder et al. (2004), support the assumption in Leuning (2000) that in relatively open canopies, the stability dependence of T_L can indeed be included via M–O based similarity functions. However, this approach seems to be reasonable only during stable conditions and more studies are needed for unstable conditions. It is logical to ask more broadly how much the atmospheric stability state in the atmospheric surface layer explains the atmospheric stability state within the canopy sublayer. We partially address this question next via a combination of model runs and data-model intercomparison.

3.2. Comparison to an analytical turbulence model

We compared the output from the analytical one-dimensional second-order closure model (Massman and Weil, 1999, hereafter MW99) to the observations using the measured foliage distribution (Fig. 1) and the parameters listed in Table 2. The value of the empirical constant for the within canopy length scale (α) was fixed to 0.06, which provided the best fit to the observed profiles of σ_i/u_*, and is consistent with the value reported by Wilson and Shaw (1977) for a range of canopy types. The upper boundary condition was fitted to the observed values of σ_i/u_* at $z/h_c = 1.47$. Fig. 8 compares the measured and modelled non-dimensional profiles of σ_u (a), σ_w (b), the shear stress (c) and the Lagrangian time scale T_L (d) in near-neutral conditions. The MW99 was able to describe the stress profile with a good accuracy throughout the stand. The model provided a good fit to the σ_u and σ_w in the trunk-space but underestimated the standard

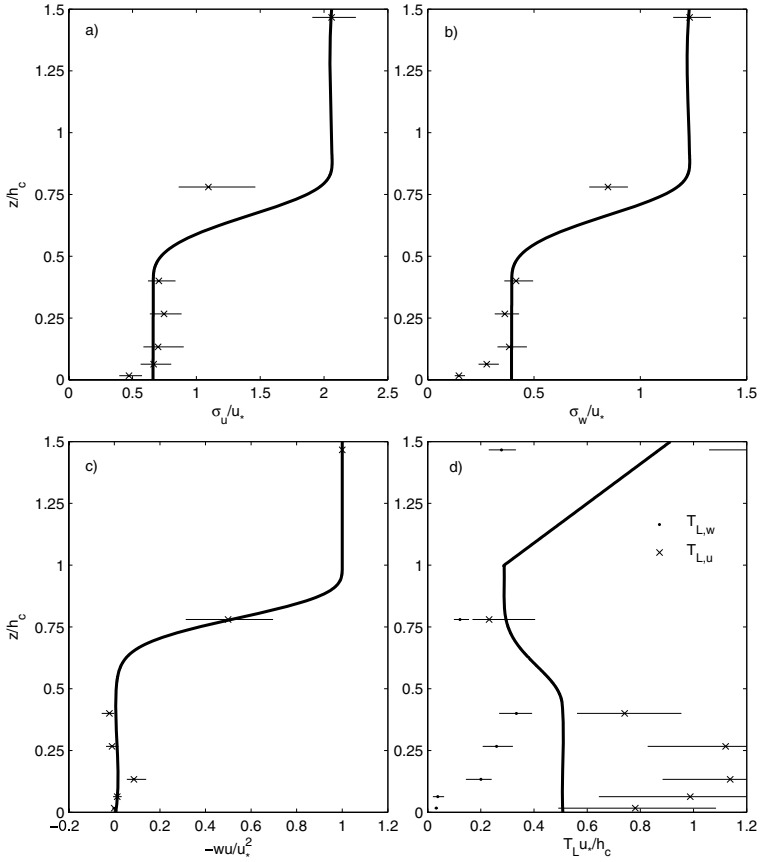

Fig. 8. Comparison of observed and modeled turbulence statistics under near-neutral conditions. Normalized standard deviations (σ_i/u_*) of u (a) and w (b), the shear stress (c) and Lagrangian time scale (d).

deviations inside the canopy crown (Fig. 8a and b). Immediately above the forest floor, the standard deviations, especially σ_w, produced by the MW99 were too large compared to the observations since the model does not assume σ_i/u_* to reach zero at the surface, which is hinted at by our observations. The T_L profile modelled using parametrizations of Massman and Weil (1999, their eq. 13 and pp. 98–99) could describe the increase in T_L in the lower part of the main canopy and in upper trunk-space but not the observed decrease at lower levels (Fig. 8d). In addition to that, the average value of the modelled T_L was significantly larger and increased faster above the canopy when compared to the observed T_{Lw}.

The MW99 assumes neutral buoyancy and therefore do not explicitly include the influence of the diabatic stability on the canopy flow equations. However, since the boundary values (σ_i/u_*) above the canopy can be either fixed to the observations or specified via standard similarity theory relationships, the stratification can be implicitly taken into account via this boundary condition. We compared the MW99 model results to the observed profiles during the various stability regimes by fitting the upper boundary to the observed values of σ_i/u_* above the canopy. We found that the MW99 described the shear stress profile well for all stability regimes except the very stable cases (data not shown). The modelled σ_i/u_* profile matched the observed profile well from the transition stable regime to near-neutral conditions. During unstable conditions, the model slightly underestimated the trunk-space values of σ_i/u_* (Fig. 4), but changing the value of α to 0.07 improved the fit. Overall, the analytical MW99 turbulence model was capable of reproducing the observed flow statistics when the upper boundary condition was adjusted to the appropriate stability regime. In short, the model-data agreement here suggests that the diabatic state of the atmospheric surface layer explains the first-order modulations inside the canopy except in the vicinity of the trunk space.

3.3. Spectral characteristics

The integral time scale analysis alone cannot reveal the existence of multiple energetic modes or describe cross-scale energy flow. For this purpose, spectral analysis is often used. We calculated the spectral densities ($P_i(f)$) using fast Fourier-transform (FFT) for detrended and Hamming-windowed (Kaimal and Kristensen, 1991) segments of ~27 min of data. Each spectrum is an average over ~3 h of daytime data collected during weakly unstable stratification ($h_c/L \sim -0.1$, $U_{22m} \sim 2.8$ ms^{-1}). Fig. 9 shows the power spectra of all three wind components and temperature against dimensionless frequency ($n = f\,h_c/U_{22m}$, bottom x-axis) and time scale (upper x-axis). The spectral densities are normalized by the variance of their respective variable.

Above the canopy, the power spectra of all the wind components and temperature (Fig. 9) follow the surface layer model spectra (Kaimal et al., 1972; Rannik et al., 1998) with a $-2/3$ slope within the inertial subrange (ISR). At the canopy crown ($0.78\ h_c$) the wind spectra steeped slightly relative to the above canopy. In the trunk-space, the spectra were distorted due to the drag imposed by the canopy elements. This distortion is often attributed to two extra processes that must be considered within the trunk space of the canopy: (1) The short-circuiting of the

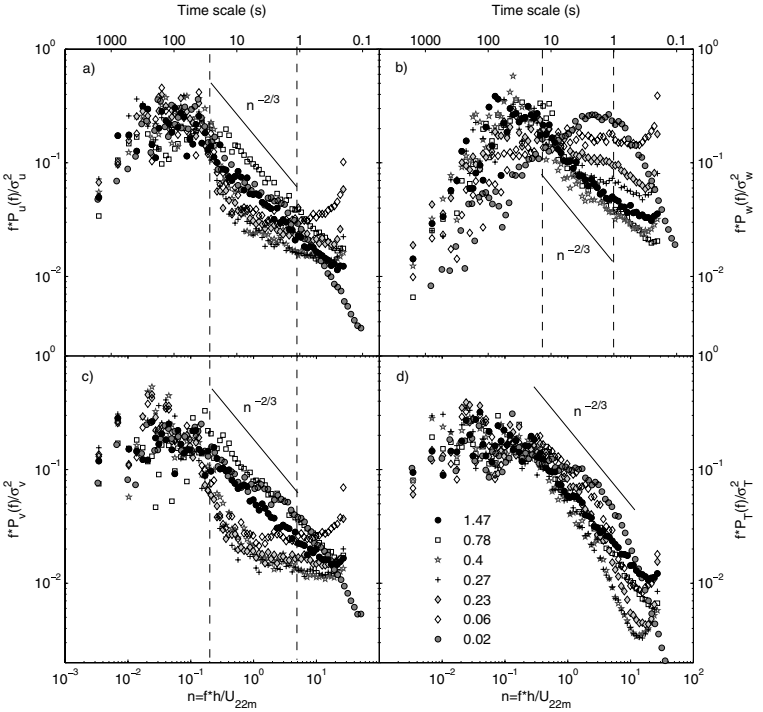

Fig. 9. Power spectra within and above forest during slightly unstable stratification ($h_c/L \sim -0.1$, $U_{22m} \sim 2.8$ ms^{-1}): u (a), w (b), v (c) and temperature (d). Different heights (z/h_c) are shown with different symbols. The vertical lines in panels (a–c) indicate the location of the inertial subrange above the canopy.

energy cascade and (2) the wake production. According to Finnigan (2000), the short-circuiting of the energy cascade impacts eddies whose size is bounded by the shear production length scale and wake production, the latter being of the order of canopy elements. Evidence of the short-circuiting in the spectra is a faster roll-off when compared to the −5/3 power law (or the −2/3 slope in the spectral representation of Fig. 9). In fact, Finnigan (2000) showed that this roll-off is given by

$$E(k) \sim k^{-5/3} \exp\left(\frac{9}{4} C_d\, a\, U\, \varepsilon^{-1/3} k^{-2/3}\right) \tag{7}$$

and approaches the $k^{-5/3}$ scaling as k increases. In the above, k is the wavenumber, C_d is the canopy drag coefficient (see Table 2), and a is the leaf area density whose vertical variation is given by Fig. 1, and ε the rate of TKE dissipation assuming the usual inertial eddy cascade. In Fig. 9, the spectral densities of the horizontal wind components in the canopy crown and in the trunk-space dropped faster at the frequencies corresponding to the low-frequency end of the inertial subrange observed above the canopy, consistent with the spectral short-circuiting model of Finnigan (2000). At high frequencies, into which the energy is converted, $P(f)$'s decreased slower than above the canopy, signaling some wake-generation. At $z/h_c = 0.78$, the leaf area density is high and it is reasonable to assume that a wake generation energy peak should be evident. However, the multiplicity of length scales (cone diameter, branches, etc.) at this level makes it impossible to discern a unique wake production length scale except perhaps at the leaf-scale. The latter scale cannot be resolved by standard sonic anemometry. The shapes of the u and v power spectra were height-independent in the trunk-space, as expected given the leaf area density profile, but the peak broadened closest to the ground ($z/h_c < 0.1$, range of n from 0.01 to 0.2). The w-component peaked at higher frequencies (range of n from 0.08 to 0.5) and behaved differently with height than the horizontal components. In the upper trunk-space ($z/h_c = 0.40$), the slope of w power spectrum was steeper than −2/3 at the low-frequency, again consistent with spectral short-circuiting and less steep at the high-frequency part of the ISR consistent with subsequent wake production. When approaching the ground, more energy was found at higher frequencies since the ground suppresses the vertical eddies and, thus, the inertial subrange was disappearing completely.

One of the most notable features in the spectra of Fig. 9, anomalous to what has been reported from earlier field experiments, is the behaviour of w power spectrum at the lowest level. Immediately above the surface ($z/h_c = 0.02$), note that the peak of the w power spectrum was shifted to significantly greater frequencies (n from 2 to 10) indicating dominance of very small vertical eddies. Similarly, a small increase in $P_w(f)$ at the other levels in trunk-space ($z/h_c < 0.5$) was observed at frequencies n from 2 to 6 (Fig. 9b), and the increase may be related to a more coherent signal of wake production in w. By using an artificial model canopy composed of rods with uniform diameter (d_r), Poggi et al. (2004a) observed unique secondary peaks in the vertical velocity power spectrum at frequencies around $fd_r/U = 0.21$. The Strouhal number 0.21 is the classical value linking the frequency of shedding of periodic von Kárman vortices with the mean flow velocity and the diameter of the obstacles (Poggi et al., 2004a). For an order of magnitude calculation to explore reasons for this increased energy at n from 2 to 10, we assume the Strouhal number ($= fd_r/U = nd_r U_{22m}/h_c U$) to be 0.21 and use a local $U \sim 0.3$ m s^{-1} observed at the lowest level. We then solve for d_r that may cause the observed peak if von Kárman vortex-like wake production dominate the energy spectrum at n from 2 to 10. With these values, we find that the d_r that may produce the observed peak frequencies, ranges from 6 to 15 cm. These values of d_r are of the same order of magnitude as the mean tree diameter ($=16$ cm), which suggests that the observed shift to higher frequencies is conceivably linked to turbulent wakes forming behind the tree trunks, while the presence of the ground destroys the larger vertical eddies. Another indirect check for the onset of von Kárman streets here is a Reynolds number comparison with the experiments of Poggi et al. (2004a) for which laser-induced florescence visualization unambiguously revealed their generation as originating from the rods (see Poggi and Katul, 2006 for detailed 2-D spectral analysis). It is known that von Kárman streets cannot be sustained at very high Reynolds number, as may have occurred at $z/h_c > 0.02$ here. Using the diameter and local velocity to define an element Reynolds number, given by $Ud_r/\nu = 0.3 \times 0.16/(1.5 \times 10^{-5}) = 3\,200$ (ν is the kinematic viscosity of air), we find that this estimate is in agreement with estimates reported in Poggi et al. (2004a). Again, the peak in n around 10 being commensurate with d_r at a moderate element Reynolds number is only a necessary but not sufficient condition for the onset of von Kárman streets generation here. When considering this von Kárman streets analogy, it is important to note that: (i) the Strouhal number used here remains constant ($=$ 0.21) and independent of the Reynolds number for a wide range of Reynolds number values (250–10 000) and (ii) the 'classical' von Kárman streets remain coherent in space only at low Reynolds number ($\sim$100), but their main instability or generation mechanism remains similar to the canopy ones in Poggi et al. (2004a) even when the Reynolds number $\sim$3 000. In terms of spatial coherency, the distance separating two 'shed' vortices is roughly $U/f = d_r/0.21 \sim 75$ cm and is smaller than the average tree-to-tree spacing (~ 3 m as described in Section 2.1). This ensures that on average at least two vortices are produced and advected before the first generated vortex collides with adjacent tree. Hence, it is likely that the spatial coherency of these vortices is limited to about 1 m before they are distorted by collisions with adjacent trees (unlike the classical Von Karman streets). Finally, there is a possibility that the peak in the w-spectrum may not only be due to vortex shedding but also due to the shallow boundary layer developing near the forest floor, whose signature is a near-logarithmic mean wind profile (U) shown in Fig. 3. The classical boundary layer mixing length is $\sim k_v z$, which at $z/h_c = 0.02$ here

is about 12 cm and not too different from the d_r. It is likely that the combined action of these two vortical motion—one based on Strouhal instability and the other based on a shallow boundary layer developing above the forest floor—caused this anomalous large peak in the w-spectrum (but not in the u or v spectra).

4. Conclusions

While there is a wealth of canopy turbulence data, synchronized multilevel flux measurements from the forest floor all the way up to the surface layer remain scarce and this scarcity motivated this experiment. We presented results from these synchronized measurements deploying five 3-D anemometers below the pine canopy, one inside the foliage and one above the canopy. The two lowest measurement levels were only 0.02 and 0.06 times the canopy height. The convenient framework for the analysis was to separate the data into four stability classes based on the classification of stability parameter (canopy height per Obukhov length) according to sensible heat flux following Mahrt et al. (1998). Using this data and classification, we explored how atmospheric stability affects (1) the bulk flow properties as well as higher-order statistics most pertinent to closure modeling, and the ejection-sweep cycle and (2) the integral time scale statistics along with modulations of the spectra. Concerning the first objective, we found that increasing atmospheric stability (i.e. from convective to stable) damped turbulent motions above and within the canopy and the influence of stability was strongest during very stable conditions when coherent structures were strongly suppressed. In a relatively open canopy, most of the observed differences in the within canopy flow in different stability regimes are related to the changes in the length scales of these dominant canopy eddies. We also found that the dimensionless TKE in the trunk space is large due to a large longitudinal velocity variance but this TKE is inactive and contributes little to momentum fluxes for all stability conditions. We have shown that the agreement between an analytical second-order closure model calculation and the data were surprisingly good despite the fact that the second-order closure model is near-neutral in formulation and admits diabatic effects only through the upper boundary conditions. With regards to the second objective, we showed that measurements of the Eulerian integral time scale do vary significantly with height and atmospheric stability. When converting these Eulerian time scale estimates to their Lagrangian equivalence, we found that $T_{Lw}\ (u_*/h_c) < 0.3$, especially in the trunk space. Implications to Lagrangian stochastic modelling approaches were discussed. Near the floor layer, a new logarithmic velocity profile is formed and vertical eddies are strongly suppressed modifying all power spectra. However, one of the surprising results was a spectral peak in the vertical velocity sampled near the ground commensurate with the trunk diameter. We showed plausible connections between this peak, the moderate element Reynolds number, and necessary conditions for generating von Kárman streets spawning off from the trunk diameter, and a shallow boundary layer developing near the forest floor.

5. Acknowledgments

We acknowledge Toivo Pohja, Erkki Siivola, Leena Järvi, Harry Lankreijer, and Tiina Markkanen for their efforts in planning and conducting the field measurements. Tiia Grönholm is acknowledged for proofreading and the two anonymous referees for their valuable comments. The study was supported by the Nordic Centre for Studies of Ecosystem Carbon Exchange and its Interactions with the Climate System (NECC).

References

Albertson, J. D., Katul, G. G. and Wiberg, P. 2001. Relative importance of local and regional controls on coupled water, carbon, and energy fluxes. *Adv. Water Resour.* **24**, 1103–1118.

Allen, L. H., Jr. 1968. Turbulence and wind spectra within a japanese larch plantation. *J. Appl. Meteorol.* **7**, 73–78.

Amiro, B. D. and Davis, P. A. 1988. Statistics of atmospheric turbulence within a natural black spruce forest canopy. *Boundary-Layer Meteorol.* **44**, 267–283.

Amiro, B. D. 1990. Comparison of turbulence statistics within three boreal forest canopies. *Boundary-Layer Meteorol.* **51**, 99–121.

Antonia, R. A. 1981. Conditional sampling in turbulence measurements. *Annu. Rev. Fluid Mech.* **13**, 131–156.

Aubinet, M., Grelle, A., Ibrom, A., Rannik, Ü., Monchrieff, J. and co-authors. 2000. Estimates of the annual net carbon and water exchange of forests: the EUROFLUX methodology. *Adv. Ecol. Res.* **30**, 113–178.

Aubinet, M., Heinesch, B. and Yernaux, M. 2003. Horizontal and vertical CO_2 advection in a sloping forest. *Boundary-Layer Meteorol.* **108**, 397–417.

Baldocchi, D. D. and Hutchison, B. A. 1988. Turbulence structure in an almond orchard: spatial vatiation in spectra and coherence. *Boundary-Layer Meteorol.* **42**, 293–311.

Baldocchi, D. D., Finnigan, J. J., Wilson, K., Paw, U. K. T. and Falge, E. 2000. On measuring net ecosystem carbon exchange over tall vegetation on complex terrain. *Boundary-Layer Meteorol.* **96**, 257–291.

Baldocchi, D. D. and Meyers, T. P. 1988a. Turbulence structure in a deciduous forest. *Boundary-Layer Meteorol.* **43**, 345–364.

Baldocchi, D. D. and Meyers, T. P. 1988b. A Spectral and lag-correlation analysis of turbulence in a deciduous forest canopy. *Boundary-Layer Meteorol.* **45**, 31–58.

Baldocchi, D. D. and Vogel, C. A. 1996. Energy and CO_2 flux densities above and below a temperate broad-leaved forest and a boreal pine forest. *Tree Physiol.* **16**, 5–16.

Bergström, H. and Högström, U. 1989. Turbulent exchange above a pine forest II: organized structures. *Boundary-Layer Meteorol.* **49**, 231–263.

Black, T. A., Den Hartog, G., Neumann, H. H., Blanken, P. D., Yang, P. C. and co-authors. 1996. Annual cycles of water vapour and carbon dioxide fluxes in and above a boreal Aspen forest. *Global Change Biol.* **2**, 219–229.

Bosveld, F. C., Holtslag, A. A. M. and Van Den Hurk, J. J. M. 1999. Nighttime convection in the interior of a dense Douglas-fir forest. *Boundary-Layer Meteorol.* **93**, 171–195.

Brunet, Y. and Irvine, M. R. 2000. The control of coherent eddies in vegetation canopies: streamwise structure spacing, canopy shear scale and atmospheric stability. *Boundary-Layer Meteorol.* **94**, 139–163.

Cajander, A. K. 1909. Ueber Wadtypen. *Acta Forestalia Fennica* **1**, 1–176 (In German).

Cava, D., Katul, G. G., Scrimieri, A., Poggi, D., Cescatti, A. and co-authors. 2006. Buoyancy and sensible heat flux budget within dense canopies. *Boundary-Layer Meteorol.* **118**, 217–240.

Chu, C. R., Parlange, M. B., Katul, G. G. and Albertson, J. D. 1996. Probability density functions of turbulent velocity and temperature in the atmospheric surface layer. *Water Resour. Res.* **32**, 1681–1688.

Cionco, R. M. 1972. Intensity of turbulence within canopies with simple and complex roughness elements. *Boundary-Layer Meteorol.* **2**, 453–465.

Dwyer, M. J., Patton, E. G. and Shaw, R. H. 1997. Turbulent kinetic energy budgets from a large-eddy simulation of airflow above and within a forest canopy. *Boundary-Layer Meteorol.* **84**, 23–43.

Feigenwinter, C., Bernhofer, C. and Vogt, R. 2004. The influence of advection on the short term CO_2-budget in and above a forest canopy. *Boundary-Layer Meteorol*. **113**, 201–224.

Finnigan, J. 2000. Turbulence in Plant Canopies. *Annu. Rev. Fluid Mech.* **32**, 519–571.

Finnigan, J. 2004. A re-evaluation of long-term flux measurement techniques Part II: coordinate systems. *Boundary-Layer Meteorol.* **113**, 1–41.

Finnigan, J., Clement, R., Malhi, Y., Leuning, R. and Cleugh, A. 2003. A re-evaluation of long-term flux measurement techniques Part I: averaging and coordinate rotation. *Boundary-Layer Meteorol.* **107**, 1–48.

Finnigan, J. and Shaw, R. H. 2000. A wind-tunnel study of airflow in waving wheat: an EOF analysis of the structure of the large-eddy motion. *Boundary-Layer Meteorol.* **96**, 211–255.

Foken, T. 2006. 50 years of Monin-Obukhov similarity theory. *Boundary-Layer Meteorol.* **119**, 431–447.

Green, S. R., Grace, J. and Hutchins, N. J. 1995. Observations of turbulent air flow in three stands of widely spaced Sitka spruce. *Agric. For. Meteorol.* **74**, 205–225.

Harman, I. N. and Finnigan, J. J. 2007. A simple unified theory for flow in the canopy and roughness sublayer. *Boundary-Layer Meteorol.* **123**, 339–363.

Hsieh, C. I., Siqueira, M., Katul, G. G. and Chu, C. R. 2003. Predicting scalar source-sink and flux distribution within a forest canopy using 2-D Lagrangian stochastic model. *Boundary-Layer Meteorol.* **109**, 113–138.

Ilvesniemi, H. and Liu, C. 2001. Biomass distribution in a young Scots pine stand. *Bor. Env. Res.* **6**, 3–8.

IPCC. 2001. In: *Climate Change 2001: The Scientific Basis, Contribution on working group I to the Third Assesment Report of the Intergovernmental Panel on Climate Change (IPCC)* (eds J. T. Houghton, Y. Ding, D. J. Griggs, M. Noguer, P. J. van der Linden and D. Xiaosu). Cambridge University Press, U.K., 1–944.

Kaimal, J. C. and Kristensen, L. 1991. Time series tapering for short data samples. *Boundary-Layer Meteorol.* **57**, 187–194.

Kaimal, J. C. and Finnigan, J. J. 1994. *Atmospheric Boundary Layer Flows: Their Structure and Measurement*. Oxford University Press, Oxford.

Kaimal, J. C., Wyngard, J. C., Izumi, Y. and Cote, O. R. 1972. Spectral characteristics of surface-layer turbulence. *Q. J. R. Meteorol. Soc.* **98**, 563–589.

Katul, G. G. and Albertson, J. D. 1998. An investigation of higher order closure models for a forested canopy. *Boundary Layer Meteorol*. **89**, 47–74.

Katul, G. G., Cava, D., Poggi, D., Albertson, J. D. and Mahrt, L. 2004. Stationarity, Homogeneity, and Ergodicity in canopy turbulence. In: *Handbook of Micrometeorology* (eds X. Lee, W. Massman and B. Law et al.). Kluwer Academic Publishers, Dordrecht, 161–180.

Katul, G. G. and Chang, W. H. 1999. Principal length scales in second-order closure models for canopy turbulence. *J. Appl. Meteorol.* **38**, 1631–1643.

Katul, G. G., Hsieh, C. I., Kuhn, G., Ellsworth, D. and Nie, D. 1997b. The turbulent eddy motion at the forest-atmosphere interface. *J. Geophys. Res.* **102**, 13409–13421.

Katul, G. G., Oren, R., Ellsworth, D., Hsieh, C. I., Phillips, N. and co-authors. 1997a. A Lagrangian dispersion model for predicting CO_2 sources, sinks and fluxes in a uniform Loblolly pine (*Pinus taeda* L.) stand. *J. Geophys. Res.* **102**, 9309–9321.

Katul, G. G., Poggi, D., Cava, D. and Finnigan, J. 2006. The relative importance of ejections and sweeps to momentum transfer in the atmospheric boundary layer. *Boundary-Layer Meteorol.* **120**, 367–375.

Kolari, P., Pumpanen, J., Kulmala, L., Ilvesniemi, H., Nikinmaa, E. and co-authors. 2006. Forest floor vegetation plays an important role in photosynthetic production of boreal forests. *Forest Ecol. Manag.* **221**, 241–248.

Kruijt, B., Malhi, Y., Lloyd, J., Nobre, A. D., Miranda, A. C. and co-authors. 2000. Turbulence statistics above and within two Amazon rain forest canopies. *Boundary-Layer Meteorol.* **94**, 297–331.

Lai, C.-T., Katul, G., Butnor, J., Ellsworth, D. and Oren, R. 2002. Modelling night-time ecosystem respiration by a constrained source optimization method. *Global Change Biol.* **8**, 124–141.

Launiainen, S., Pumpanen, J., Mölder, M., Kulmala, L., Lankreijer, H. and co-authors. 2006. Vertical variations in fluxes and turbulence characteristics within a forest – a joint NECC-campaign in Hyytiälä, Southern Finland. In: *Proceeding of BACCI, NECC and FcoE activities 2005 book B*, *Report Series in Aerosol Sciences 81A* (eds M. Kulmala, A. Lindroth and T. M. Ruuskanen). Helsinki, Finland.

Launiainen, S., Rinne, J., Pumpanen, J., Kulmala, L., Kolari, P. and co-authors. 2005. Eddy covariance measurements of CO_2 and sensible and latent heat fluxes during a full year in a boreal pine forest trunk-space. *Bor. Environ. Res.* **10**, 569–588.

Law, B. E., Kelliher, F. M., Baldocchi, D. D., Anthoni, P. M., Irvine, J. and co-authors. 2001. Spatial and temporal variation in respiration in a young ponderosa pine forest during a summer drought. *Agric. For. Meteorol.* **110**, 27–43.

Leclerc, M. Y., Beissner, K. C., Shaw, R. H., Den Hartog, G. and Neumann, H. H. 1990. The influence of atmospheric stability on the budgets of the reynolds stress and turbulent kinetic energy within and above a deciduous forest. *J. Appl. Meteorol.* **29**, 916–933.

Leclerc, M. Y., Beissner, K. C., Shaw, R. H., Den Hartog, G. and Neumann, H. H. 1991. The influence of buoyancy on third-moment

turbulent velocity statistics within a deciduous forest. *Boundary-Layer Meteorol.* **55**, 109–123.

Lee, X. 2000. Air motion within and above forest vegetation in non-ideal conditions. *Forest Ecol. Manag.* **135**, 3–18.

Lee, X. and Black, T. A. 1993a. Atmospheric turbulence within and above a Douglas-fir stand. Part I: statistical properties of the velocity field. *Boundary-Layer Meteorol.* **64**, 149–174.

Lee, X. and Black, T. A. 1993b. Atmospheric turbulence within and above a Douglas-fir stand. Part II: eddy fluxes of sensible heat and water vapour. *Boundary-Layer Meteorol.* **64**, 369–389.

Lee, Y.-H. and Mahrt, L. 2005. Effect of stability on mixing in open canopies. *Agric. For. Meteorol.* **135**, 169–179.

Legg, J. B., Raupach, M. R. and Coppin, P. A. 1986. Experiments on scalar dispersion within a model plant canopy. Part III. An elevated line source. *Boundary-Layer Meteorol.* **35**, 277–302.

Leuning, R. 2000. Estimation of scalar source/sink distributions in plant canopies using Lagrangian dispersion analysis: corrections for atmospheric stability and comparison with a multilayer canopy model. *Boundary-Layer Meteorol.* **96**, 293–314.

Lien, R.-C. and D'Asaro, E. 2002. The Kolmogorov constant for the Lagrangian velocity spectrum and structure function. *Phys. Fluids* **14**, 4456–4459.

Loescher, H. W., Ocheltree, T., Tanner, B., Swiatek, E., Dano, B. and co-authors. 2005. Comparison of temperature and wind statistics in contrasting environments among different sonic anemometer-thermometers. *Agric. For. Meteorol.* **133**, 119–139.

Mahrt, L., Lee, X., Black, A., Neumann, H., Staebler, R. M. 2000. Nocturnal mixing in a forest subcanopy. *Agric.For. Meteorol.* **101**, 67–78.

Mahrt, L., Sun, J., Blumen, W., Delany, T. and Oncley, S. 1998. Nocturnal boundary-layer regimes. *Boundary-Layer Meteorol.* **88**, 255–278.

Markkanen, T., Rannik, Ü., Marcolla, B., Cescatti, A. and Vesala, T. 2003. Footprints and fetches for fluxes over forest canopies with varying structure and density. *Boundary-Layer Meteorol.* **106**, 437–459.

Massman, W. J. and Weil, J. C. 1999. An analytical one-dimensional second-order closure model of turbulence statistics and the Lagrangian time scale within and above plant canopies of arbitrary structure. *Boundary-Layer Meterorol.* **91**, 81–107.

Mölder, M., Klemedtsson, L. and Lindroth, A. 2004. Turbulence characteristics and dispersion in a forest – tests of Thomson's random-flight model. *Agric. For.Meteorol.* **127**, 203–222.

Novak, M. D., Warland, J. S., Orchansky, A. L., Ketler, R. and Green, S. 2000. Wind tunnel and field measurements of turbulent flow in forests. Part I: uniformly thinned stands. *Boundary-Layer Meteorol.* **95**, 457–495.

Peltola, A. 2001. *Metsätilastollinen vuosikirja* (Finnish Statistical Yearbook of Forestry). Finnish Forest Research Institute, Vammala. (In Finnish).

Poggi, D. and Katul, G. G. 2006. Two-dimensional scalar spectra in the deeper layers of a dense and uniform model canopy. *Boundary Layer Meteorol.* **121**, 267–281.

Poggi, D., Katul, G. G. and Albertson, J. D. 2004b. Momentum transfer and turbulent kinetic energy budgets within a dense model canopy. *Boundary-Layer Meteorol.* **111**, 589–614.

Poggi, A., Porporato, A., Ridolfi, L., Albertson, J. D. and Katul, G. G. 2004a. The effect of vegetation density on canopy sub-layer turbulence. *Boundary-Layer Meteorol.* **111**, 565–587.

Poggi, D., Katul, G. G. and Albertson, J. D. 2006. Scalar dispersion within a model canopy: measurements and three-dimensional Lagrangian models. *Adv. Water Resour.* **29**, 326–335.

Pumpanen, J., Launiainen, S., Kulmala, L., Järvi, L., Markkanen, T. and co-authors. 2006. Nighttime CO_2 storages below forest canopy estimated from continuous CO_2 concentration profile measurements with NDIR-based CO_2 probes. In: *Proceeding of BACCI, NECC and FcoE activities 2005 book B, Report Series in Aerosol Sciences 81B* (eds M. Kulmala, A. Lindroth and T. M. Ruuskanen). Helsinki, Finland.

Rannik, Ü. 1998. On the surface layer similarity at a complex forest site. *J. Geophy. Res. D* **103**, 8685–8697.

Rannik, Ü., Markkanen, T., Raittila, J., Hari, P. and Vesala, T. 2003. Turbulence inside and over Forest: influence on Footprint Prediction. *Boundary Layer Meteorol.* **109**, 163–189.

Raupah, M. R. 1989. Applying Lagrangian fluid mechanics to infer scalar source distributions from concentration profiles in plant canopies. *Agric. For. Meteorol.* **47**, 85–108.

Raupach, M. R., Coppin, P. A. and Legg, B. J. 1986. Experiments on scalar dispersion within a model plant canopy, Part I: the turbulent structure. *Boundary-Layer Meteorol.* **35**, 21–52.

Raupach, M. R., Finnigan, J. J. and Brunet, Y. 1996. Coherent eddies and turbulence in vegetation canopies: the mixing-layer analogy. *Boundary Layer Meteorol.* **78**, 351–382.

Raupach, M. R. and Thom, A. S. 1981. Turbulence in and Above Plant Canopies. *Annu. Rev. Fluid Mech.* **13**, 97–129.

Shaw, R. H. 1977. Secondary Wind Speed Maxima Inside Plant Canopies. *J. Appl. Meteorol.* **16**, 514–521.

Shaw, R. H., Den Hartog, G. and Neumann, H. H. 1988. Influence of foliar density and thermal stability on profiles of Reynolds stress and turbulence intensity in a deciduous forest. *Boundary-Layer Meteorol.* **45**, 391–409.

Siqueira, M., Lai, C. T. and Katul, G. G. 2000. Estimating scalar sources, sinks, and fluxes in a forest canopy using Lagrangian, Eulerian, and Hybrid inverse models. *J. Geophys. Res.* **105**, 29475–29488.

Staebler, R. M. and Fitzjarrald, D. R. 2004. Observing subcanopy CO_2 advection. *Agric. For. Meteorol.* **122**, 139–156.

Stenberg, P., Palmroth, S., Bond, B. J., Sprugel, D. G. and Smolander, H. 2001. Shoot structure and photosynthetic efficiency along the light gradient in a Scots pine canopy. *Tree Physiol.* **21**, 805–814.

Strong, C., Fuentes, J. D. and Baldocchi, D. D. 2004. Reactive hydrocarbon flux footprints during canopy senescence. *Agric. For. Meteorol.* **127**, 159–173.

Su, H.-B., Shaw, R. H. and Paw, U. K.T. 2000. Two-point correlation analysis of neutrally stratified flow within and above a forest from large-eddy simulation. *Boundary-Layer Meteorol.* **49**, 423–460.

Suni, T., Rinne, J., Rannik, Ü., Reissell, A., Altimir, N. and co-authors. 2003. Long-term measurements of surface fluxes above a Scots pine forest in Hyytiälä, southern Finland, 1996-2001. *Bor. EnvIRON. Res.* **8**, 287–302.

Taylor, G. I. 1921. Diffusion by continuous movements. *Proc. London Math. Soc.* **20**, 196–212.

Tennekes, H. 1979. Exponential Lagrangian correlation-function and turbulent-diffusion in the inertial subrange. *Atmos. Environ.* **13**, 1565–1567.

Thomson, D. J. 1987. Criteria for the selection of stochastic models of particle trajectories in turbulent flows. *J. Fluid Mech.* **180**, 529–556.

Yi, C., Monson, R. K., Zhai, Z., Anderson, D. E., Lamb, B. and co-authors. P. 2005. Modeling and measuring the nocturnal drainage flow in a high-elevation, subalpine forest with complex terrain. *J. Geophys. Res.* **110**, D22303, doi:10.1029/2005JD006282.

Vesala, T., Haataja, J., Aalto, P., Altimir, N., Buzorius, G. and co-authors. 1998. Long-term field measurements of atmosphere-surface interactions in boreal forest combining forest ecology, micrometeorology, aerosol physics and atmospheric chemistry. *Trends Heat, Mass Momentum Transfer* **4**, 17–35.

Vesala, T., Suni, T., Rannik, Ü., Keronen, P., Markkanen, T. and co-authors. 2005. The effect of thinning on surface fluxes in a boreal forest. *Global Biogeochem. Cycl.* **19**, GB2001, doi:10.1029/2004GB002316, 2005.

Villani, M. G., Schmid, H. P., Su, H.-B., Hutton, J. L. and Vogel, S. 2003. Turbulence Statistics Measurements in Northern Hardwood Forest. *Boundary-Layer Meteorol.* **108**, 343–364.

Wesson, K. H., Katul, G. G. and Siqueira, M. 2003. Quantifying organization of atmospheric turbulent eddy motion using nonlinear time series analysis. *Boundary-Layer Meteorol.* **106**, 507–525.

Wilson, N. R. and Shaw, R. H. 1977. A higher-order closure model for canopy Flow. *J. Appl. Meteorol.* **16**, 1197–1205.

Zhang, H., Chen, J. and Park, S.-U. 2001. Turbulence structure in unstable conditions over various surfaces. *Boundary-Layer Meteorol.* **100**, 243–261.